Corrosion of Conductor Rolls in the Electrogalvanizing Line at Ternium Siderar

Walter Egli[1], Pablo Seré[2], Leandro Bengoa[2], Florencia Versino[2],
Sonia Bruno[3], Andrés Lazzarino[4], Fernando Espósito[4]

(1. Researcher of CICPBA-CIDEPINT, La Plata, Argentina;
2. Facultad de Ingeniería, Universidad Nacional de La Plata, La Plata, Argentina;
3. REDE-AR Tenaris Siderca, Campana, Argentina;
4. Ternium Siderar, Florencio Varela, Argentina)

Abstract: Conductor rolls in the electrogalvanizing line are made of Duplex Stainless Steel (DSS) and after some time in service they suffer surface deterioration leading to surface defects and rejections in high quality products. Repassivation kinetics and susceptibility to pitting corrosion for the austenitic and ferritic phases were studied. An electrochemical treatment that reproduces the actual industrial corrosive situation was applied to test different alloys in the laboratory. The Hastelloy C22 showed the best performance and was evaluated in the line during a complete production batch. The new roll presented a slight deterioration, much lower than the DSS rolls.

Key words: corrosion, conductor roll, electrogalvanizing

1   Introduction

Conductor rolls in the electrogalvanizing line at Ternium Siderar are made of Duplex Stainless Steel (DSS) SAF2205 and after some time in service they suffer surface deterioration and uneven dissolution. This process has been considered as a corrosion-erosion phenomenon, it produces a pattern on the roll surface that is transferred to the electrogalvanized material leading to surface defects and rejections in high quality products. The DSS rolls usually start affecting the product's surface quality after rolling for 3 or 4 days and the process starts very quickly when 2 faces material is produced.

The line has 10 horizontal cells with catalytic anodes, maximum current density is 90 A/dm^2, the electrolyte is a mixture of zinc sulphate, sodium sulphate and sulphuric acid, pH is 1.9 and working temperature is 60-65°C.

The DSS has good mechanical properties and high corrosion resistance in very aggressive media, but the differences in composition and morphology of the phases austenitic and ferritic can affect its performance. Some studies show that galvanic corrosion or intergranular corrosion can appear [1-3].

The material selection criteria for conductor roll construction are usually based in some standards, while very exigent for corrosion resistance evaluation of alloys in oxidant media, they do not represent the actual situation of this application [4-7]. A cyclic anodic current treatment that accelerates the corrosive attack on stainless steel and other alloys has been proposed but this is not the real behaviour of a conductor roll connected to the cathode of an electrochemical system [8]. Townsend et al. presented a more realistic cyclic connection and disconnection of zinc electrodes to stainless steel but without in field validation of the correct electrochemical potentials [9].

Egli et al. measured the electrochemical potential of roll and strip surfaces during operation in the electrogalvanizing line. In this way, the real corrosive conditions of the rolls were evaluated and an electrochemical cyclic treatment was designed [10]. This treatment was used to generate the same type of corrosion pattern that was observed in the DSS. Different alloys were tested in the laboratory and the Hastelloy C22 electrodes showed the best performance.

Based on these results, one conductor roll was made of C22 and evaluated in the electrogalvanizing line during one complete production batch. The resulting

wear was measured comparing with SAF2205 rolls. Some laboratory tests were also performed using single phase austenitic and ferritic electrodes to give some insight on the corrosion mechanism.

2   Experimental method

2.1   Working electrodes

A sample of a discarded conductor roll was cut. The lateral faces and back of small blocks of 1 cm^2 section were isolated with acrylic polymer, polished with different abrasive papers and finally given a mirror finish with 1 μm diamond paste.

Electrodes of single phase austenitic (γ) and ferritic (α) where made by selective anodic dissolution of each phase of the SAF2205 with the technique developed by Tsai [1]. A monophasic ferritic electrode (MFE) was obtained dissolving austenite at −0.257V and a monophasic austenitic electrode (MAE) was generated dissolving ferritic phase at −0.341 V. In Fig. 1 both electrodes are shown. This was confirmed by microscopy and EDS analysis: austenite appears as islands in a continuous ferritic matrix [4].

A Hastelloy C22 2 mm diameter rod was cut and included in araldite polymer and the same polishing treatment as for SAF2205 sample was applied. Some pieces of the C22 new roll were cut and similar electrodes were built. In Table 1 chemical compositions of the working electrodes are presented.

2.2   Electrochemical tests

The electrochemical experiments were carried out in a conventional three-electrode cell thermostatized at (50 ±0.5)ºC operated with an EG&G Princeton Applied Research Potentiostat/Galvanostat (Mod. 273A) coupled to a personal computer equipped with the CorrWare2 software for data acquisition and control. The temperature was selected in analogy with the industrial process. A saturated HgSO$_4$ RE was used in all the experiences to avoid chloride contamination of the electrolyte. All potentials reported here are expressed in volts (V) with respect to SCE (+0.241 V vs. SHE). A platinum foil of 10 cm^2 area was used as counter electrode. The working electrolyte was an aqueous solution having ZnSO$_4$ (90 g/L Zn^{2+}) at 1.6 pH.

A modification of Park and Kwon scratch test was used to study repassivation kinetics by electrochemical reduction of the passive layer in DSS, MFE and MAE electrodes [3].

2.3   Plant trial with C22 new roll

The new roll was put in the line for one normal production cycle that lasted 1 month. At the end of the cycle, the C22 roll was taken out of the line altogether with the damaged DSS rolls. Silicone and acetate replicas were prepared to characterize the worn surfaces.
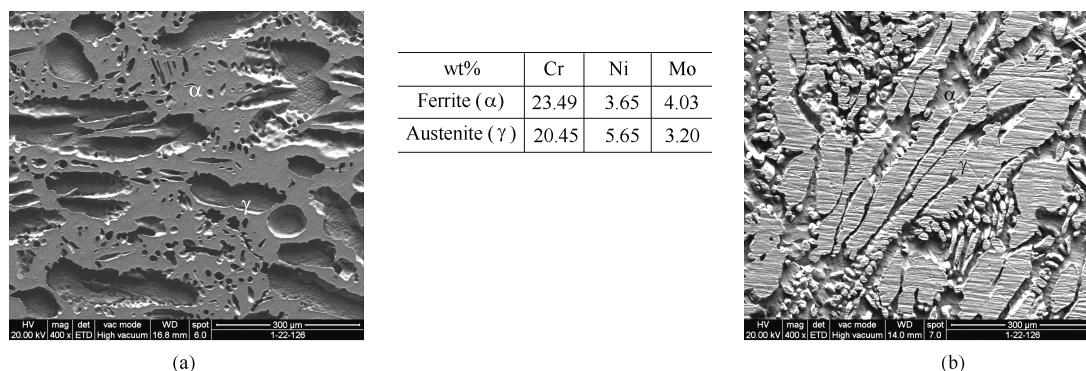

wt%	Cr	Ni	Mo
Ferrite (α)	23.49	3.65	4.03
Austenite (γ)	20.45	5.65	3.20

Fig.1   Monophasic electrodes, 400×

(a)Monophasic ferritic electrode; (b)Monophasic austenitic electrode

Table 1   Chemical compositions of working electrodes

	Ni	Cr	Fe	Mo	C$_{max}$	N	Co$_{max}$	W
SAF 2205	5	22	bal	3.2	0.03	0.18	—	—
Hastelloy C22	bal	20-22.5	2.0-6.0	12.5-14.5	0.01	—	2.5	3.0

2.4 Microscopy

An USB microscope was used to examine the surface of the rolls on site. SEM microscopy (Quanta200 FEI with Tungsten filament source) plus EDS analysis was used to characterize the electrode surfaces before and after the cyclic treatments. The electrodes topography and the roll surface replicas were characterized with a digital optical 3D high resolution microscopy (HIROX KH-7700).

3　Results and discussion

3.1　Potential cycling

The electrochemical potential of SAF2205 and C22 conductor rolls (E_r) and the galvanized strip (E_{st}) in contact with them were measured for different operating conditions and for different product specifications using the system described by Egli et al. [10]. The results showed that the same values of electrochemical potential were obtained for both types of roll materials. This experimental fact supported the application of potential cycling as a corrosion performance predictive technique.

Considering that a roll takes τ s to fulfil a complete revolution and that t_c is the contact time between the sheet and the roll, an asymmetric repetitive square wave potential (ARSW) signal like the one described in Fig.2 was applied. In this case, the electrode surface stay $(\tau-t_c)$ s at E_r and t_c s at E_{st}. So, each ARSW cycle represents electrochemically one revolution of a conductor roll.

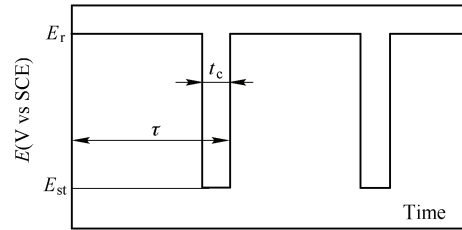| Product	E_r	E_{st}
1 face	−0.3	−0.7
2 faces	−0.4	−1.4

Fig.2　Asymmetric repetitive square wave potential signal

The parameter τ is directly related to line speed and roll diameter and t_c depends on line speed and contact length between conductor roll and strip. The roll-strip contact length was measured with pressure sensitive polymeric film for different roll pressures and diameters taking 0.05 cm as a representative average value. Using the actual set of conductor rolls diameter and the real line speeds for the production mix it was possible to take t_c=0.01s and τ=1.5 s as representative average values. The resulting ARSW with these characteristic times was applied to the SAF2205 electrode for 30 min (1200 cycles) adjusting E_r and E_{st} to the measured values for the 2 faces material. A strong corrosion pattern appeared with clear evidence of differential attack of duplex grain structure and pitting (Fig. 3).
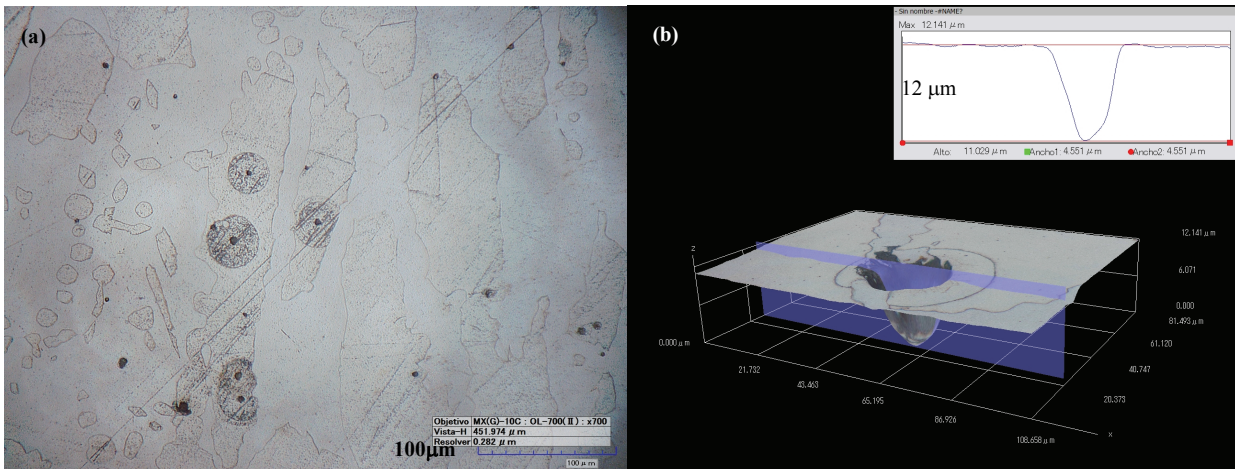

Fig. 3　3D optical images of SAF2205 electrode after ARSW treatment

(a) General view; (b) Pit detail

Pitting appeared mostly in the austenitic phase or between austenite and ferrite grain boundaries. It was observed that in these working conditions the austenitic phase is more susceptible to pitting than the ferritic phase.

Hastelloy C22 rod and C22 roll electrodes showed no evidence of corrosion after 30 min of cyclic treatment. Longer ARSW treatments were applied to the C22 samples and after 2 h a very light evidence of pitting appeared (Fig. 4).
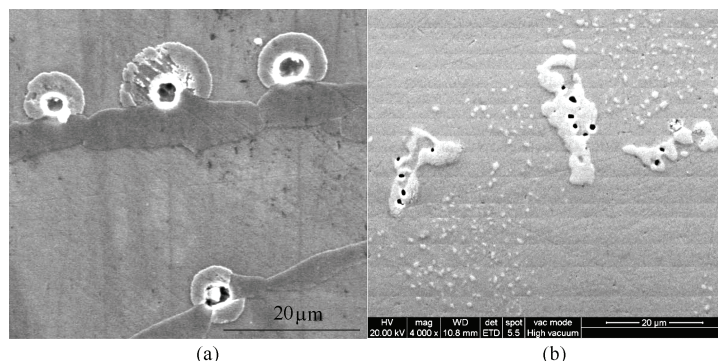

(a)   (b)

Fig. 4 SEM images of ARSW treatment

(a) SAF2205 (1000 ×), 30 min ARSW ; (b) C22 (4000×), 2 h ARSW

3.2 Repassivation kinetics

Cabrera and Mott used the high field ionic conduction model to explain passive layer formation in stainless steels; the passive layer grows by metallic ions transport through it towards the solution interface under the effect of a strong electric field [11]. It was demonstrated that when a passive layer is disrupted (scratch test), a linear relationship exists between the logarithm of the anodic current density that circulates to reconstruct the system and the inverse of the charge density:

$$\log i \, (t) = A + cBV / q(t)$$

A and *B* are related to the activation energy for ions migration, *V* is the voltage drop in the interface and *c* is a constant that depends on the alloy. The slope value *cBV* is a measure of the repassivation rate of an alloy in a determined media. The lower *cBV* value for a specific system, the higher repassivation rate for the alloy, producing a thinner and more protective passive layer during the repassivation process [12] .

Considering this model, repassivation kinetics for the SAF 2205, MAE and MFE were measured and the slope *cBV* was calculated (Table 2).

Table 2   *cBV* for SAF 2205 and monophasic electrodes

	cBV /cm^2·C^{-1}	Correlation factor
SAF 2205	0.00138	0.98
MFE	0.00096	0.95
MAE	0.00191	0.95

It could be said the main difference in the corrosion mechanism between both roll materials is the dual phase structure of SAF2205 steel and the different kinetic depassivation and repassivation of ferrite and austenite phases. In the case of C22 alloy this effect is absent.

3.3   Evaluation of worn rolls surface

The surface of the conductor rolls after one complete production cycle was characterized and digital in situ micrographs were obtained. The general appearance of both types of rolls is shown in Fig. 5. A severe attack is observed on the SAF2205 conductor roll surface and a very peculiar strips pattern is detected on the C22 roll.

The changes in diameter of the rolls after the production cycle were evaluated. Wear was calculated as the difference between the average initial diameter and the final diameter measured in the centre of the roll. In Table 3 results are shown for two SAF2205 rolls (A and B) and the C22 roll. Wear for the C22 roll was less than for the DSS rolls.

The silicone replicas showed that in SAF2205 valleys of about 25 μm deep were formed, whereas in the C22 roll strips of attacked and non-attacked zones were observed. The corroded zones showed higher roughness but the whole surface was flat (Fig. 6).
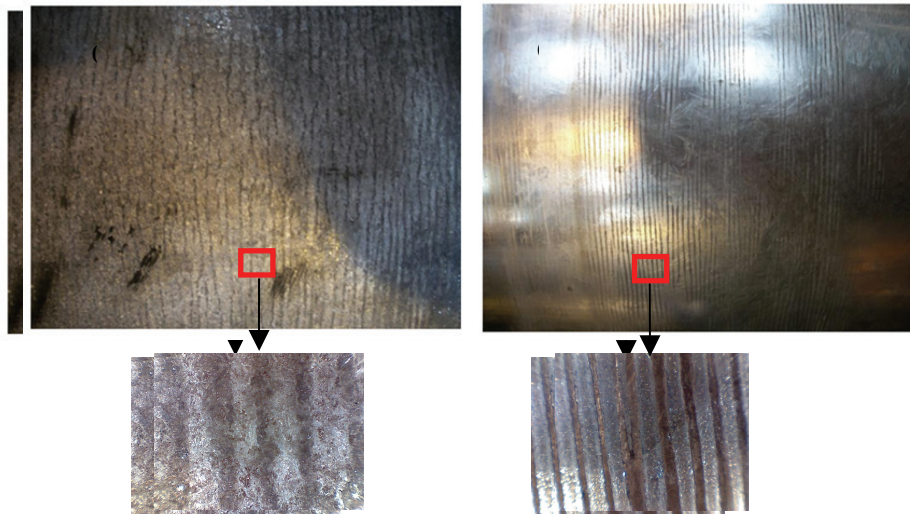
Fig. 5   Worn rolls, top image without magnification and bottom image at 200×
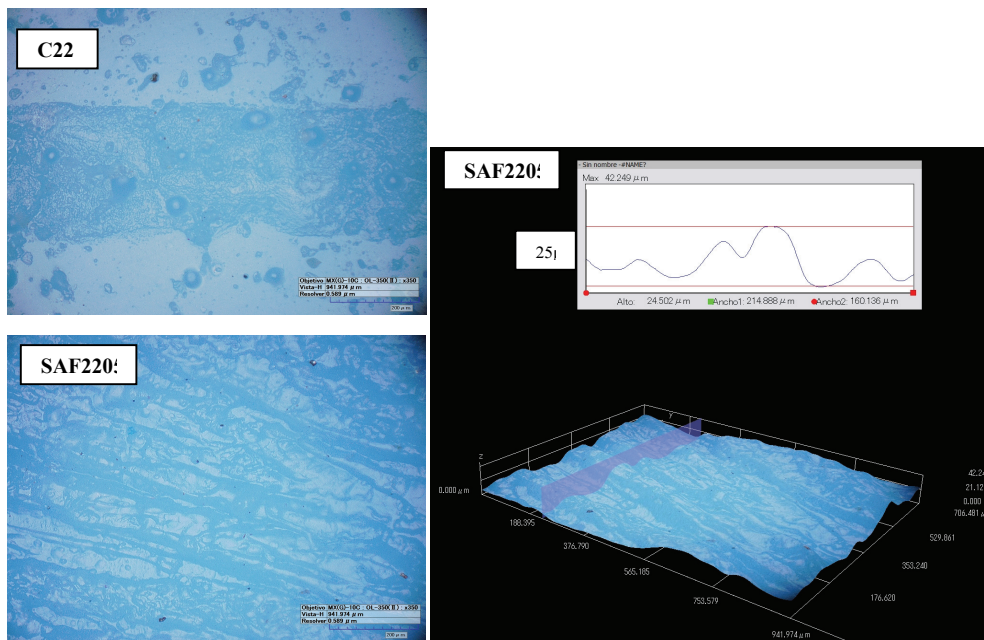
(a) SAF2205; (b) C22

Fig. 6   Worn rolls, silicone replicas

Table 3   Comparative wear

Roll	Wear/mm
SAF 2205 (A)	0.85
SAF 2205 (B)	0.61
C22	0.27

4   Conclusions

(1) The potential cycling method allowed to test the different alloys and to choose C22 for making the new roll.

(2) This roll was tested in the line showing less corrosion and wear than the currently used SAF2205 rolls.

(3) The studies with monophasic electrodes allowed to understand corrosion mechanisms for DSS: austenitic phase acts as anode and ferritic phase as cathode.

(4) Both materials C22 and SAF2205 suffer pitting corrosion but this process is much more severe for the last one.

References

[1] Wen-Ta Tsai, Jhen-Rong Chen. Galvanic Corrosion Between the Constituent Phases in Duplex Stainless Steel. Corrosion Science 49 (2007): 3659–3668.

[2] Femenia M., Pan J., Leygraf C., Luukkonen P. In Situ Study of Selective Dissolution of Duplex Stainless Steel 2205 by Electrochemical Scanning Tunneling Microscopy. Corrosion Science 43 (2001): 1939–1951.

[3] Chan-Jin Park, Hyuk-Sang Kwon. Effects of Aging at 475ºC on Corrosion Properties of Tungsten-Containing Duplex Stainless Steels. Corrosion Science 44 (2002): 2817–2830.

[4] Uhlig's Corrosion Handbook, 2nd Edition by R. Winston Revie, John Wiley & Sons Inc., 2000.

[5] Shreir L.L. Corrosion. Vol 1 - Metal Environment Reactions 3rd Ed. Shreir, Jarman & Burstein, 1994.

[6] Asm Handbook. Vol. 13B, Corrosion: Materials, 2005.

[7] Asm Handbook, Vol. 13C, Corrosion: Environments and Industries, 2006.

[8] Rebak R. Laboratory Testing to Evaluate the Corrosion Performance of Conducting Roll Materials in the Electroplating Industry, CORROSION 97, paper No. 264, 1997.

[9] Townsend H., Steinbicker R., Yau Y. Corrosion of Stainless Steel Conductor Rolls in a Continuous Sheet Electrogalvanizing Line. Corrosion Vol. 46 (1990), No. 5: 418–423.

[10] Egli W., Seré P., Bruno S., Lazzarino A. Corrosion of Conductor Rolls in an Electrogalvanizing Line. Procedia Materials 00 (2011).

[11] Cabrera N., Mott N.F. Theory of the Oxidation of Metals. 1949 Rep. Prog. Phys. 12 163.

[12] Eun-Ae Cho, Chin-Kwan Kim, Joon-Shick Kim, Hyuk-Sang H. Kwon. Quantitative Analysis of Repassivation Kinetics of Ferritic Stainless Steel Based on the High Field Ion Conduction Model. Electrochemical Acta 45 (2000): 1933–1942.